Chapter 6

Design Optimization, Thermo-hydraulic, and Enviro-economic Analysis of Twisted Perforated tape Insert-based Heat Exchanger with nanofluid using CFD and TGM

In this chapter, passive inserts, the effect of perforated twisted tape insert (PTTI)-based heat exchanger (HX) utilizing hybrid nanofluid as working fluid undercooling, turbulent flow model has been investigated. In the present numerical analysis, PTTI of various perforated pitches and perforation sizes at different operating conditions kept well aligned in a tube with hybrid nanofluid (Al_2O_3-CuO-TiO_2-H_2O) as a coolant medium (hot fluid being cooled) at 0.12% (v/v) is investigated. This numerical study aims to address the swirling flow generated by the tapes for different geometrical conditions to evaluate the heat transfer enhancement in terms of Nusselt ratio and Friction ratio (FR). Enviro-economic analysis has also been investigated for different PTTI in HX. Turbulent flow analysis has been investigated under constant tube wall temperature with a 2mm to 4mm perforation size at three different perforated pitches under other flow conditions. Furthermore, Taguchi-Grey analysis has been studied to obtain the effect of geometric and operating parameters conditions to optimize the heat transfer, minimize the pressure drop, and predict the prioritized set of geometrical and fluid flow conditions. Input parameters required for the Taguchi-Grey analysis are determined from the CFD (Computational fluid dynamics).

6.1 Physical Model

Knowledge of complex turbulence fluid flow behavior is crucial for heat transfer enhancement. This study utilizes CFD results to optimize the considered HX geometry. The

detailed design configuration of the tube inserted with perforated twisted tape is presented in Fig. 6.1 and listed in Table 6.1. Fixed dimensions are twisted tape pitch (P_t = 85mm), length of tube (L = 340mm), width of tape (W_t = 6mm), tape thickness (t_t = 1mm), tube inner diameter (D_i = 8mm), tube outer diameter (D_o = 9mm), twist ratio (P_t/W_t = 14.2). Three different perforated pitches of three different perforated diameters of circular shape have been investigated at different operating conditions. In this research study, hot fluid, also termed coolant fluid (which is being cooled), nanofluid of (volume concentration = 0.0012) composition as a working fluid [**Kumar et al. 2021.].** The fluid flows along the z-direction of the cartesian coordinate. The thermophysical properties of water and alumina are illustrated in Table 6.2.

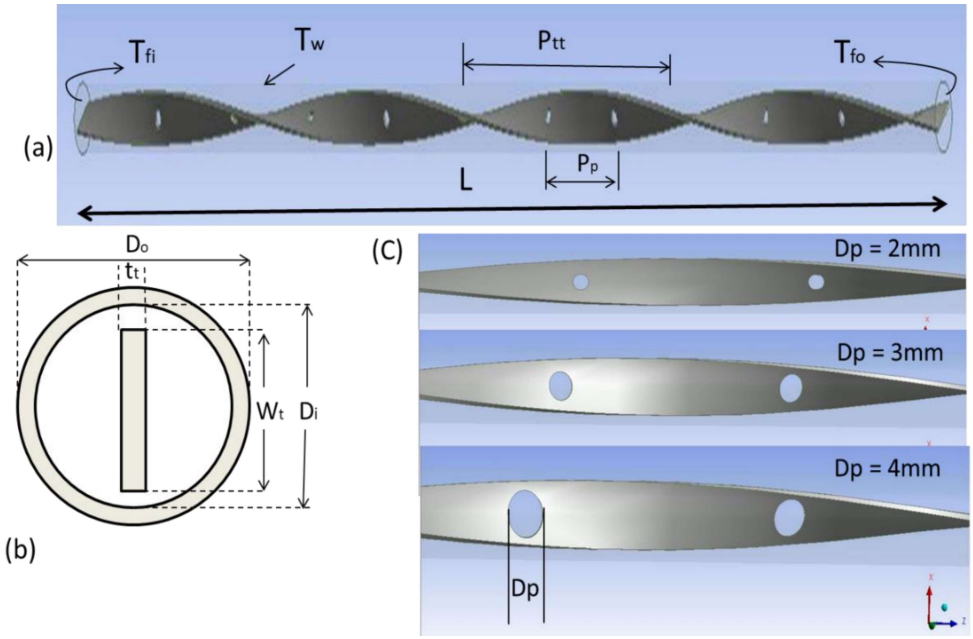

Fig. 6.1. Physical model, (a) geometry of plain tube with perforated twisted tape inserts; (b) cross-section; (c) twisted tapes of 2, 3, and 4mm perforated diameter.

Geometry is prepared in the workbench module of Ansys 16.0 design modular. Prepared geometry has meshed as unstructured tetrahedron meshing elements of the mesh. The number of divisions method is used to generate a refined mesh for further increment in the number of factors

in the vicinity of the perforated twisted tape and tube inner diameter. Meshed model of the plain tube with PTTI of 30mm perforated pitch and 3mm perforated diameter is depicted in Fig. 6.2.

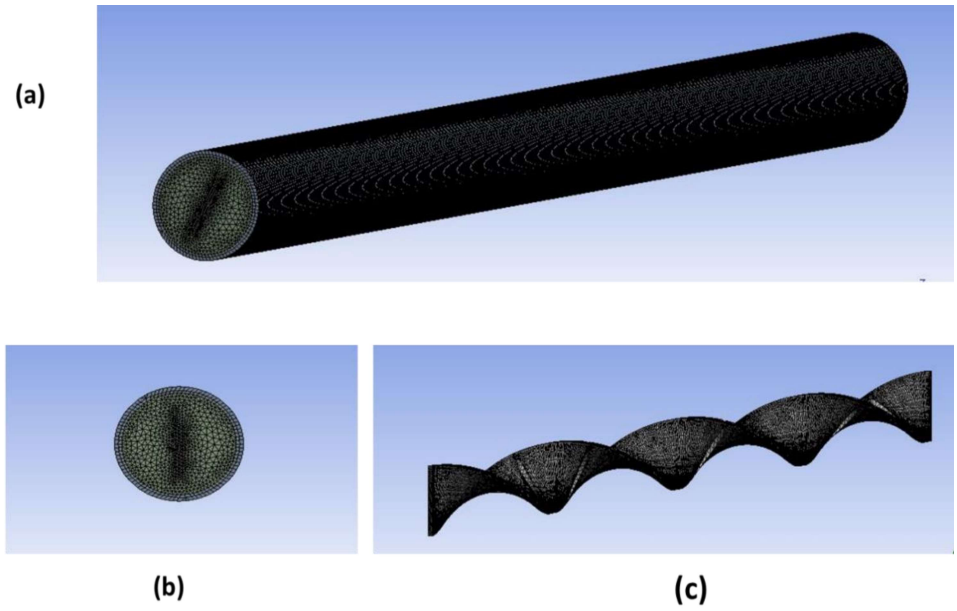

Fig. 6.2. Grid generated, (a) Meshed model of full geometry; (b) Cross-section of the tube; (c) Perforated twisted tape meshed.

Table. 6.1 Detailed dimension of perforated twisted tape inserts.

Perforated pitch (P_p) [mm]	**Perforated diameter (D_p) [mm]**	**P_p/P_{tt}**	**Porosity S_p (%)**	**Number of perforations (N)**
20	2	0.25	2.6	17
	3	0.25	5.8	17
	4	0.25	10.5	17
30	2	0.35	1.65	11
	3	0.35	3.8	11
	4	0.35	6.7	11
40	2	0.50	1.25	8
	3	0.50	2.6	8

	4	0.50	4.9	8

Table. 6.2 Thermo-physical properties of the working fluid.

Properties	Water	Al_2O_3	CuO/TiO_2	Hybrid nanofluid
Specific heat capacity (c_p) [J/kg-K]	4181	765	531/711	4162
Thermal conductivity (k)[W/m-K]	0.6303	40	18/4.8	0.661
Viscosity (μ)[kg/m-s]	0.00066	_____	_____	0.00084
Prandtl Number (Pr)	4.38	_____	_____	5.2
Density (ρ) [kg/m^3]	988	3970	6310/4170	1025

6.2 Mathematical model and numerical technique

6.2.1 *Governing equations*

A three-dimensional (3D) computational model is generated for simulations. Assumptions are employed in the current numerical investigation. Nanofluid as a working fluid is incompressible, with the flow fully developed turbulent regime and internal tube diameter used as the hydraulic diameter for calculation. The equations of continuity, momentum, and energy equation to solve in turbulent regime with working fluid as nanofluid can be modeled as;

$$\frac{\partial(u_i)}{\partial x_i} = 0, \text{ Continuity equation} \tag{6.1}$$

$$\frac{\partial}{\partial x_j}\left(u_i u_j \rho_{nf}\right) = -\frac{\partial p}{\partial x_i} + \frac{\partial}{\partial x_j}\left(-\rho_{nf}\overline{u_j' u_i'}\right) + \frac{\partial}{\partial x_j}\left(\mu_{nf}\left(\frac{\partial u_i}{\partial x_j} + \frac{\partial u_j}{\partial x_i}\right)\right), \text{ Momentum equation} \tag{6.2}$$

$$\frac{\partial}{\partial x_i}\left(T\rho_{nf}u_i\right) = \frac{\partial}{\partial x_i}\left(\left(\frac{\mu_{nf}}{\mathrm{Pr}_{nf}} + \frac{\mu_{tc}}{\mathrm{Pr}_{tc}}\right)\frac{\partial T}{\partial x_i}\right), \text{ Energy equation} \tag{6.3}$$

where $\rho_{nf}\overline{u_j' u_i'}$ and μ_{tc} estimated as;

$$-\rho_{nf}\overline{u_j' u_i'} = \mu_{tc}\left(\frac{\partial u_i}{\partial x_j}+\frac{\partial u_j}{\partial x_i}\right)-\frac{2}{3}\rho_{nf}k\delta_{ij}-\frac{2}{3}\mu_{tc}\frac{\partial u_k}{\partial x_k}\delta_{ij} \tag{6.4}$$

$$\mu_{tc}=\frac{\rho_{nf}C_\mu k^2}{\varepsilon},\ \mathrm{Pr}_{nf}=\frac{\mu_{nf}c_{p,nf}}{k_{nf}}$$

k, Ɛ are estimated as;

$$\frac{\partial}{\partial x_j}\left(\left(\frac{\mu_{tc}}{\sigma_k}+\mu_{nf}\right)\frac{\partial k}{\partial x_j}\right)-\rho_{nf}\varepsilon+G_k=\frac{\partial}{\partial x_i}\left(u_i\rho_{nf}k\right),\ \text{where}\ G_k=-\frac{\partial u_j}{\partial x_i}\rho_{nf}\overline{u_j' u_i'} \tag{6.5}$$

$$\frac{\partial}{\partial x_i}\left(u_i\rho_{nf}\varepsilon\right)=\frac{\partial}{\partial x_j}\left(\left(\frac{\mu_{tc}}{\sigma_\varepsilon}+\mu_{nf}\right)\frac{\partial \varepsilon}{\partial x_j}\right)+\frac{\varepsilon}{k}G_k C_{1\varepsilon}-\rho_{nf}\frac{\varepsilon^2}{k}C_{2\varepsilon} \tag{6.6}$$

Where constants are $C_{1\varepsilon}$ = 1.42, $C_{2\varepsilon}$ = 1.68, σ_ε = 1.3, σ_k = 1 , C_μ = 0.0845, Pr_{tc} = 0.85

The finite volume method is analyzed, and the simulation is solved in Ansys fluent solver 16.0. For analysis, volume concentration (ϕ = 0.0012) and thermo-physical properties of the hybrid nanofluid ρ_{nf}, μ_{nf}, k_{nf}, $c_{p,nf}$ are listed in Table 6.2. Now heat transfer enhancement coefficient for the above geometrical configuration compared to a plain tube is defined as the Nusselt ratio (NR). For different perforated twisted tape inserts, heat transfer improvement compared to the plain tube can be estimated as follows;

$$NR=\frac{\left(Nu_{nf}\right)_{PTTI}}{\left(Nu_{nf}\right)_{PT}} \tag{6.7}$$

Due to the use of various perforated twisted tape inserts, improvement of heat transfer occurs at the rise in the penalty in pressure drop. Relative pressure drop coefficients for different PTTI are defined as Friction ratio (FR) and estimated as;

$$FR=\frac{\left(ff_{f,nf}\right)_{PTTI}}{\left(ff_{f,nf}\right)_{PT}} \tag{6.8}$$

Overall thermal performance (OTP) combines heat transfer and pressure penalty for power consumption. For practical application of PTTI in HX at an equal power supply can be expressed as follows;

$$OTP = \frac{NR}{(FR)^{\left(\frac{1}{3}\right)}} \tag{6.9}$$

PTTI of different geometry considered in heat exchanger enhance heat transfer but at the cost of pumping power. CO_2 discharge will be a significant criterion for analysis in terms of power requirement for a heat exchanger. Carbon emissions utilization can be claimed with CO_2 discharge. CO_2 discharge [**Caliskan et al. 2012**] is calculated as;

$$DG_{CO_2} = \frac{f_{CO_2} PP_{Net} t_{run}}{10^6} \tag{6.10}$$

Where $PP_{net} = \frac{\Delta p \dot{m}}{\rho \eta_p}$,pump efficiency (η_p) is taken as 65%, DG_{CO_2} is the discharge of carbon to the environment in tonnes per year. PP_{net} the net power consumption in kW required to run the heat exchanger for an hour f_{CO_2} represents the carbon discharge factor. The carbon discharge factor is 0.82kgCO_2/kWh (Location-based) [**Kashyap et al. 2020**] and t_{run} is the annual running time (h/Annum). The operational cost of the PTTI in a heat exchanger using net electricity consumption is evaluated as;

$$HX_{OC} = PP_{Net} t_{run} C_{electricity} \tag{6.11}$$

Data analysis is evaluated by assuming heat exchangers run continuously for eight hours a day and 365 days a year before maintenance. The electricity price ($C_{Electricity}$) is considered as 8 per kWh.

Overall heat transfer coefficient (UA), considering both internal fluids as nanofluid and external fluid as air for the heat exchanger for analysis of heat transfer enhancement, is calculated by;

$$\frac{1}{UA} = \frac{1}{h_a A_a} + \frac{1}{h_f A_f} + \frac{\ln(\frac{D_0}{D_i})}{2\pi L k_t} + \frac{t_t}{k_t A_{tt}} \tag{6.12}$$

Where A_a is the outer surface area of the tube, A_f is the tube's internal surface area, and A_{tt} is the area of the twisted tape. For the investigation, outer fluid air flows at a velocity of 5m/s [**Kumar et al. 2022**].

6.2.2 Boundary conditions

Tube and perforated twisted tape materials are considered aluminium. Nanofluid is a hot working fluid circulated inside the tube with inlet temperature (T_{fi} = 343K). The tube wall is employed at isothermal conditions (T_w = 313K). Although isothermal conditions are difficult to achieve, constant temperature is assigned for HX analysis to cool the hot fluid [**Goudarzi et al. 2017**]. The entry velocity of fluid is 0.35, 0.45, 0.55, 0.65, and 0.75m/s assigned corresponding to mass flow rate of 0.018, 0.023, 0.028, 0.033, and 0.038kg/s (Reynolds number 3800 – 8150) respectively at the inlet section of tube, while outlet section is specified as pressure outlet condition. The tube length is more than ten times the hydraulic diameter [**Slichting 1979**]. Since the total tube length is 340mm, and the hydraulic diameter of the considered geometry is 8mm, thus ensuring a fully developed flow. Automatic mesh with some divisions at the tube wall and PTTI vicinity refined mesh is generated for the computational domain. Tube walls and PTTI have the effects of conduction. The inner surface of the tube and PTTI surface are assigned as no-slip boundary conditions.

6.2.3 Numerical technique

In the present investigation, the Reynolds number is beyond 2000. Therefore, the turbulent model is adopted. RNG k-Ɛ model solves the continuity, momentum, and energy equation in Ansys fluent solver. Turbulent models are generally classified as zero, one, and two-equation models. Two-equation eddy viscosity models are preferred in twisted tape analysis, as listed in Table 6.3.

Table. 6.3 Models investigated for twisted tape analysis.

Author	Modified twisted tape	Turbulent model investigated
Saedodin et al., [2020]	Twisted tape inserts	k-ω
Kola et al., [2021]	u-cut twisted tape inserts	k-Ɛ standard wall treatment
Eiamsaard et al., [2009]	Loose fit TTI	SST k-ω
Abed et al., [2018]	v- cut TTI	k-Ɛ Realizable
Li et al., [2018]	Helically twisted tape insert	RNG k-Ɛ

The RNG (Renormalization group) k-Ɛ model includes swirl flow in turbulence, is sensitive to flow separation and recirculation, and considers effective viscosity even at a low Reynolds number. Therefore, in the present investigation, the RNG k-Ɛ model is preferred over the standard k-Ɛ model, provided a finer mesh near-wall region. Scale residual of 10^{-6} assigned to continuity and energy for convergence. For momentum, 10^{-5} is specified as the convergence criteria. Detailed solution technique for solver setting, spatial discretization, and solution method selection in the present numerical study is listed in Table 6.4.

Table. 6.4 Solution method settings applied in ANSYS FLUENT.

Solver	Steady-state, pressure-based solver	
Viscous model	RNG k-Ɛ model	
Solution method	Pressure velocity coupled	Semi implicit pressure linked equation, SIMPLE

	Gradient	Green-Gauss node based
	Pressure	Standard
Discretization	Momentum	Second-order upwind
	Turbulent kinetic energy	Second-order upwind
	Turbulent dissipation rate	Second-order upwind

6.2.4 Grid independence study

The smaller size of the cells usually measures model correctness, and the output becomes independent of grid size; this is called a grid independence study. In general mesh, independence starts with a coarse mesh and then to the refined mesh till independent data is achieved. Five different grids are generated on a PTTI of 20mm perforated pitch and 4mm perforated diameter configuration utilizing nanofluid as a flow medium at a mean velocity of 0.35m/s. The number of cells is around $4.53*10^5$, starting with coarse mesh, then gradually refining the mesh of $11.42*10^5$, $15.65*10^5$, $20.73*10^5$, and $25.95*10^5$. Nu and *ff* are estimated with grid variation presented in Fig. 4.3., and up to $15*10^5$ grid, considered coarser to the medium grid, variation in Nu and ff data are large. Both Nu and *ff* value shows an insignificant difference when grid numbers are beyond $15.65*10^5$. The difference in Nu was 0.13% and 0.28% when grids increased from $20.73*10^5$ to $25.95*10^5$, ensuring data is independent of the number of the grid. Thus, $20.73*10^5$grids are selected in the present investigation.

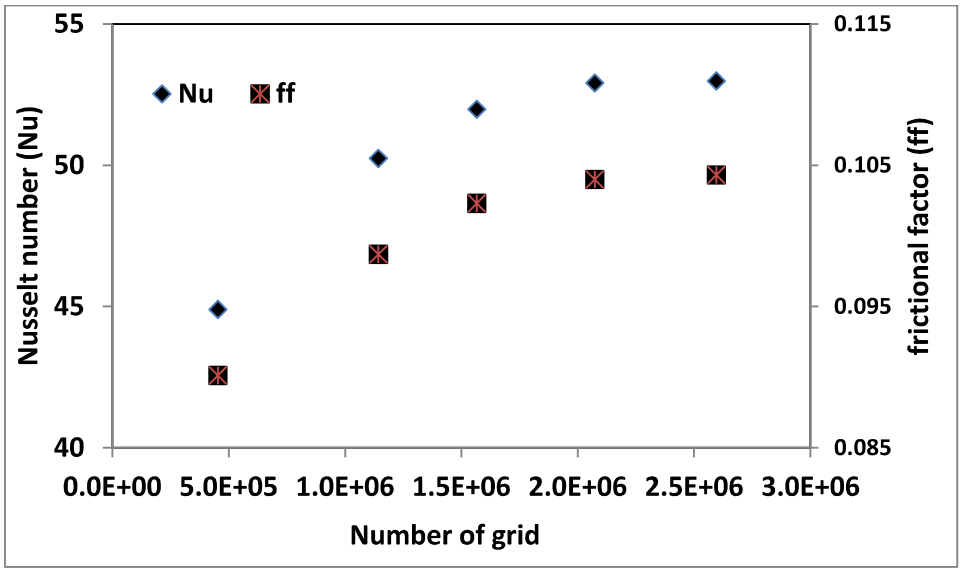

Fig. 6.3. Graphical presentation of grid independence test, **(a)** Nu; **(b)** frictional factor.

6.2.5 Numerical verification and validation

For comparison, CFD has determined the Nusselt number and frictional factor for a plain tube, with water as a working medium. The present numerical study accuracy is compared with the theoretical correlations and available experimental results within the same working range, as shown in Fig. 6.4.

The non-dimensional Nusselt number and frictional factor is given as,

$$Nu = \frac{h_f * D_h}{k_f}$$, where h is heat transfer coefficient (W/m^2.K), D_h is hydraulic diameter (m) and k_f is thermal conductivity of fluid (W/m^2.K). (6.13)

$$ff = \frac{2 * \Delta p * D_h}{L * \rho_f * V^2}$$, where L is tube length (m), ρ is density (kg/m^3), V is fluid velocity (m/s) (6.14)

The theoretical Gnielinski Nusselt number is given as,

$$Nu = \left[\left(\mathrm{Re}_f - 1000 \right) \times \mathrm{Pr}_f \times 0.5 \times \left(\frac{ff}{1 + 12.7 \times \left(\mathrm{Pr}_f^{2/3} - 1 \right) \times \left(\frac{f_f}{2} \right)^{0.5}} \right) \right], \text{ where Pr is Prandtl} \quad (6.15)$$

number, and $\mathrm{Re_f}$ is fluid Reynolds number.

Petukhov equation for frictional factor is given as,

$$ff = \left[1.58 \times \ln(\mathrm{Re}_f) - 3.28 \right]^{-2}, 0.5 < pr_f < 2000, 3000 < \mathrm{Re}_f < 5000000 \quad (6.16)$$

The Dittus-Boelter equation for Nusselt number is given as,

$$Nu = 0.023 * \mathrm{Re}_f^{0.8} * Pr^{0.3}, \quad 0.6 < pr_f < 16, \mathrm{Re}_f > 10000 \quad (6.17)$$

Blasius equation for frictional factor is given as,

$$ff = (0.79 \ln \mathrm{Re}_f - 1.64)^{-2} .5 < pr_f < 160, 2300 < \mathrm{Re}_f < 5 * 10E6 \quad (6.18)$$

$ff = 0.316 \mathrm{Re}_f^{-0.25}$, frictional factor for Developed turbulent flow (6.19)

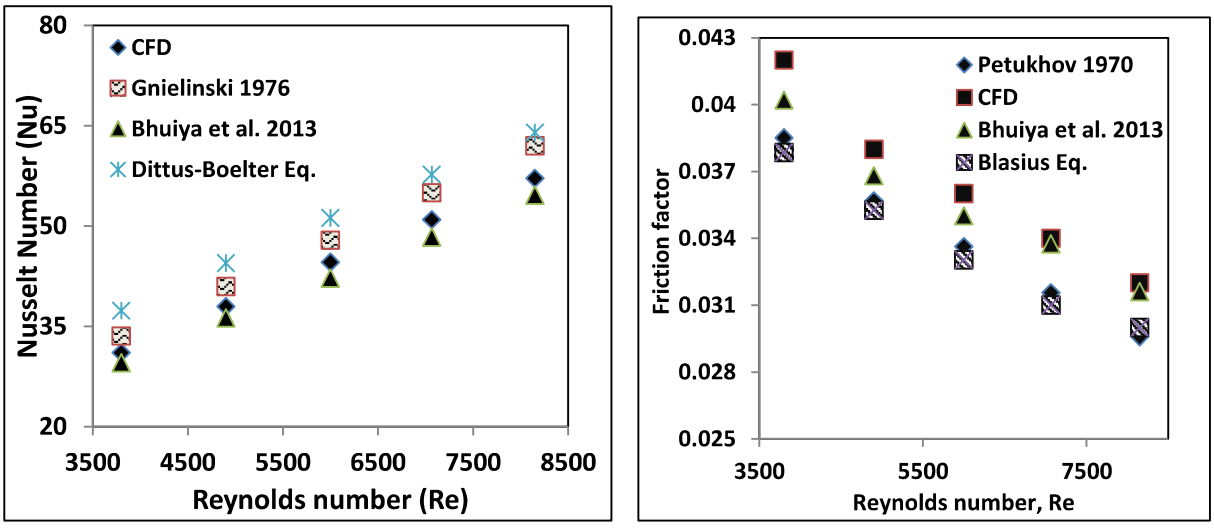

(a) (b)

Fig. 6.4. Verification of plain tube, (a) Nu with Re; (b) frictional factor with Reynolds number.

For Nusselt number, see Fig. 6.4.(a), theoretical results obtained from the Gnielinski 1976, correlation , Dittus-Boelter Eq. (6.17) for cooling of fluid, and experimental results of **Bhuiya et**

al. 2013 are compared to the computational results with water as fluid flow. For frictional factor, CFD results are compared to the Petukhov, 1970, shown in Eq. (6.16), Blasius Equation given in Eq. (6.18), and available similar experimental results as shown in Fig. 6.4. (b). It is obtained that CFD data agree with the functional theoretical correlations, and the RNG k-Ɛ model predicted the experimental result. Numerical results of the Nusslet number have shown adequate accuracy with the Gnielinski theoretical correlation and with the experimental results of Bhuiya et al. 2013. Nusselt number shows the maximum deviation of 17.13% with the D-B equation, 5.4% with Bhuiya, and 8.4% with Gnielinski correlations. The numerical prediction of the friction factor deviates a minimum of 2.5% and a maximum of 8.8% with the theoretical correlation. The experimental results of **Bhuiya et al. 2013** are well predicted, and the maximum error of the experimental results, Nusselt number $\pm 5.4\%$ and for frictional factor $\pm 5.0\%$, and the CFD results are obtained well within the error range.

6.2.6 Optimization technique

The orthogonal simulated plan was obtained from the design factors and their levels. Perforated pitch, perforated size, and mass flow rate are the design factors of the three levels listed in Table 6.5. Planned simulation runs to obtain the target response, pressure drop, and HTC. The SN (Signal to Noise) ratio is determined per the target response's objective. The larger the best is determined as;

$$SN = 10\log_{10}\left[\frac{1}{n}\sum_{i=1}^{n}\frac{1}{Y_i^2}\right] \tag{6.20}$$

And for smaller the best, the equation is;

$$SN = 10\log_{10}\left[\frac{1}{n}\sum_{i=1}^{n}Y_i^2\right] \tag{6.21}$$

Where Y_i is the performance value of their individual and n presents the total run.

$$N_i(j) = \frac{\max x_i(j) - x_i(j)}{\max x_i(j) - \min x_i(j)} \text{ (larger value is better.)} \tag{6.22}$$

$$N_i(j) = \frac{x_i(j) - \max x_i(j)}{\max x_i(j) - \min x_i(j)} \text{ (smaller the better.)} \quad (6.23)$$

Where N_i (j) represents the normalization response (0 to 1) and $x_i(j)$ is the original comparative sequence. And i = 1,2,3……., n and j = 1,2,3……,m. Where n is the total runs and m is the total responses. The simulated results are normalized in the range of 0 to 1 as per the target response (heat transfer and pressure drop). Now, The GRC (Grey relational coefficient) is determined for each run as;

$$GRC = \frac{D_{min} + \Psi * D_{\max}}{D_{oi}(j) + \Psi * D_{\max}} \quad (6.24)$$

D_{min} and $D_{\max}$ represents the minimum and maximum value of the absolute difference of a comparing sequence, respectively. Ψ represents the identification or distinguish coefficient for the real systems requirements 0.5 [**Wang et al., 2016; Pandey et al., 2017; Naquiddin et al., 2018**.]. D_{oi} represents the deviation of the reference and the identical sequence.

For multiple responses, the Grey relational grade (GRG) is determined as;

$$GRG = \frac{\sum_{j=1}^{m} GRC}{m} \quad (6.25)$$

Table. 6.5 Design factors and their levels.

Factor		Level		
		1	2	3
A	Perforated pitch (P_p), [mm]	20	30	40
B	Perforated diameter (D_p),[mm]	2	3	4
C	Mass flow rate ($\dot{m}$), [kg/s]	0.018	0.028	0.038

6.3 Results and discussion

6.3.1 Effect of flow and geometrical parameters on heat transfer

The flow field across a tube with perforated twisted tape inserts is more complex than the plain tube. The purpose of the PTTI is to enhance the heat transfer of the heat exchanger. Figs.

6.5.-6.6. shows the temperature contour at six different cross-sections along the axial direction of the tube with inserts. Hybrid nanofluid enters at a higher temperature T_{fi} = 343K and loses its temperature to the wall kept at a lower temperature. Temperature contour reveals that fluid temperature reduces continuously along the axial direction of the fluid flow. For PTTI, D_p = 4mm and P_p = 20mm; at the lower Reynolds number, 3800, defines lower mass flow rate, swirl flow, and lower inertia allow the fluid to have a higher resident time of fluid mixing near the wall and the twisted surface, thus ensuring the larger temperature drop of fluid, for instance (see in Fig. 6.5). In contrast, the resident time reduces with the increased flow rate,

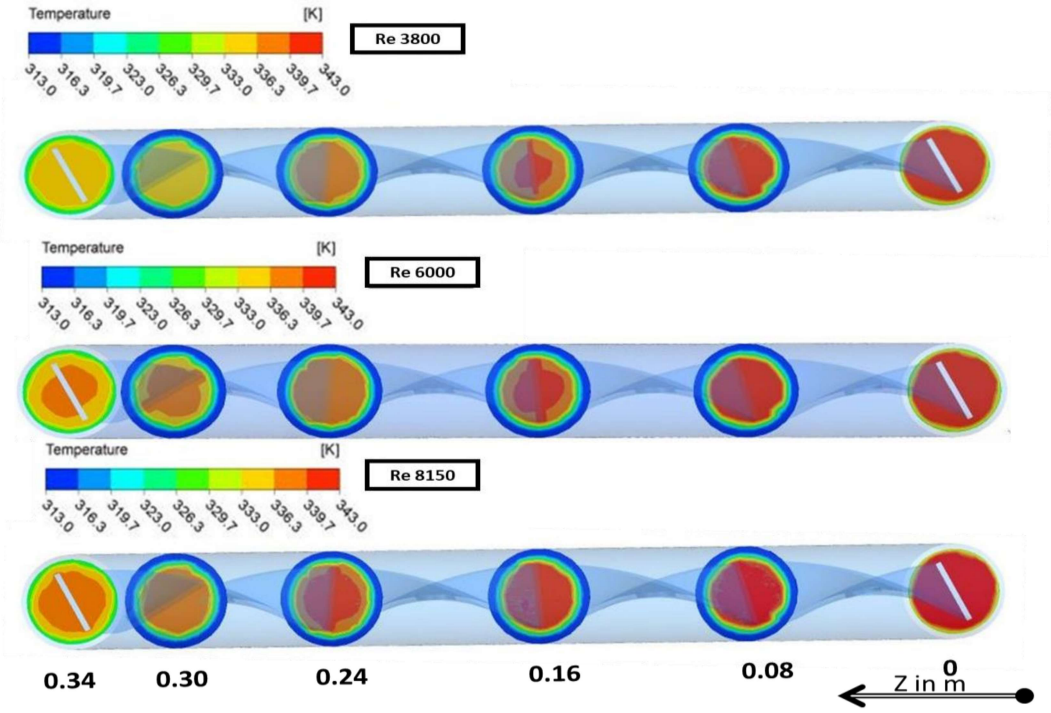

Fig. 6.5. Temperature contours along the flow direction at different Reynolds number.

and therefore, the temperature drop also reduces. The effect of perforated pitch on the fluid temperature in temperature contour at different sections along the longitudinal direction of fluid flow with a fixed flow rate of 0.018kg/s (3800 Reynolds number) and D_p of 4mm is presented in Fig. 6.6. A lower perforated pitch allows more perforations, as each perforation causes disruption in fluid flow and regenerates the secondary flow for further temperature reduction. Due to this

reason, the lowest perforated pitch causes the highest temperature reduction, and the temperature drop reduces with the increased perforated pitch.

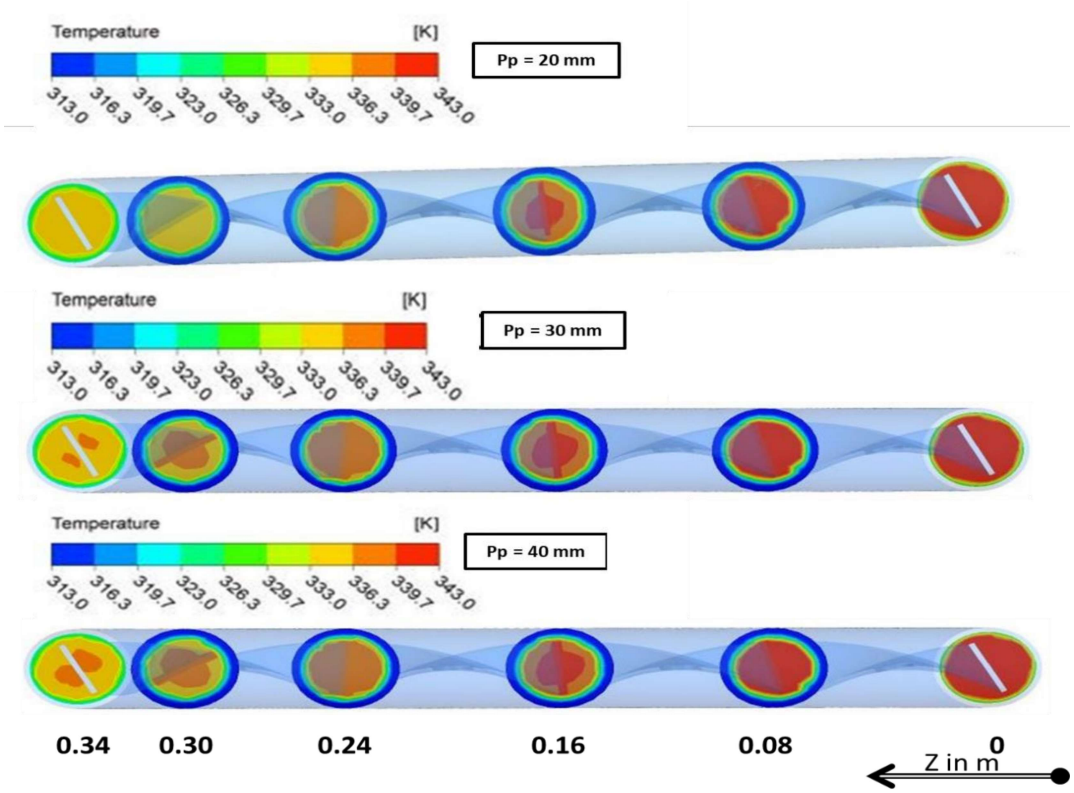

Fig. 6.6. Temperature contours along the flow direction with a perforated pitch.

The purpose of this heat exchanger is to cool the hot fluid rapidly. Perforated diameter creates further turbulence, and a larger diameter allows fluid to regenerate the boundary layer and increases local turbulence at a higher internal diameter, thus resulting in a potential geometrical parameter for temperature reduction and heat transfer enhancement. The lowest fluid outlet temperature is obtained at the lowest Re of 3800 for perforated geometrical conditions of D_p 4mm, P_p 20mm, and a maximum overall temperature drop of 3.1°C is obtained at the lowest Reynolds number minimum drop of 2.7°C at the highest Reynolds number with geometrical conditions variation. However, Fig. 6.7 shows the Nusselt ratio for different geometrical shapes of PTTI in HX with the Reynolds number. Nusselt ratio shows higher than unity for all cases studied, ensuring better modification in heat transfer enhancement than the plain tube. Nusselt ratio decreases with

the increased Reynolds number due to axial flow dominance over swirling flow effects. Lower fluid mass flow rate, fluid velocity, and Reynolds number are better sets of fluid conditions as influential parameters for the larger temperature reduction in the case of PTTI in HX. Geometrical parameters perforated pitch and perforated diameter also influence the heat transfer enhancement ratio.

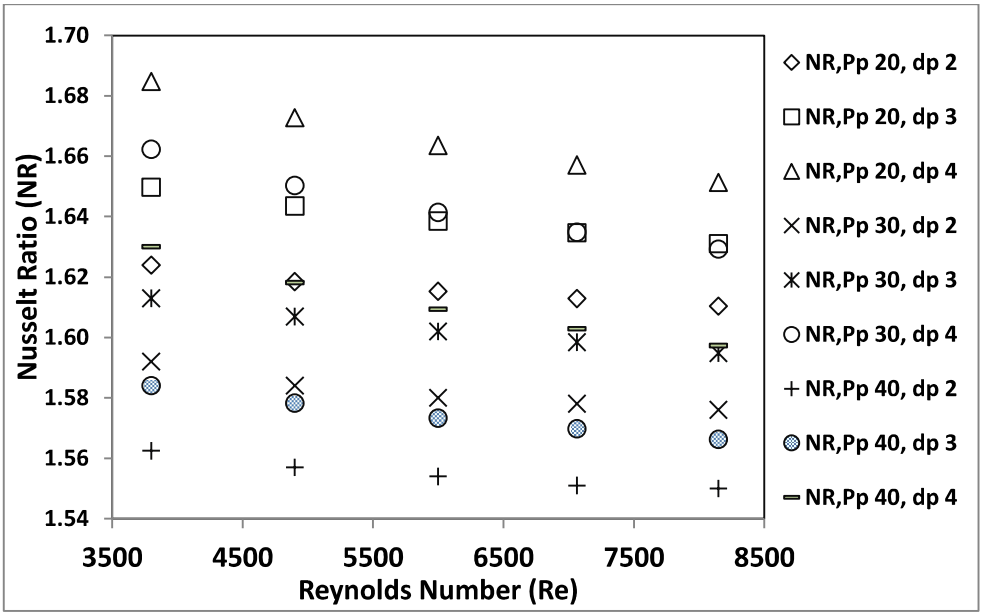

Fig. 6.7. Nusselt ratio with Reynolds number under different PTTI conditions.

Lower perforated pitch and higher perforated diameter show the highest Nusselt ratio at each Reynolds number. Lower perforated pitch causes a higher number of perforations, resulting in more recirculation points generated near the vicinity of perforation, thus causing higher temperature reduction. Also, a perforated diameter regenerates the fluid flow, and a larger diameter shows higher enhancement. However, PTTI in HX shows 68.5% higher enhancement at the lowest flow rate. With the geometrical and fluid flow variation conditions of PTTI in HX, the Nusselt number enhancement ratio ranges from 55.5% to 68.5% higher compared to the plain tube.

6.3.2 Effect of flow and geometrical parameters on pressure drop

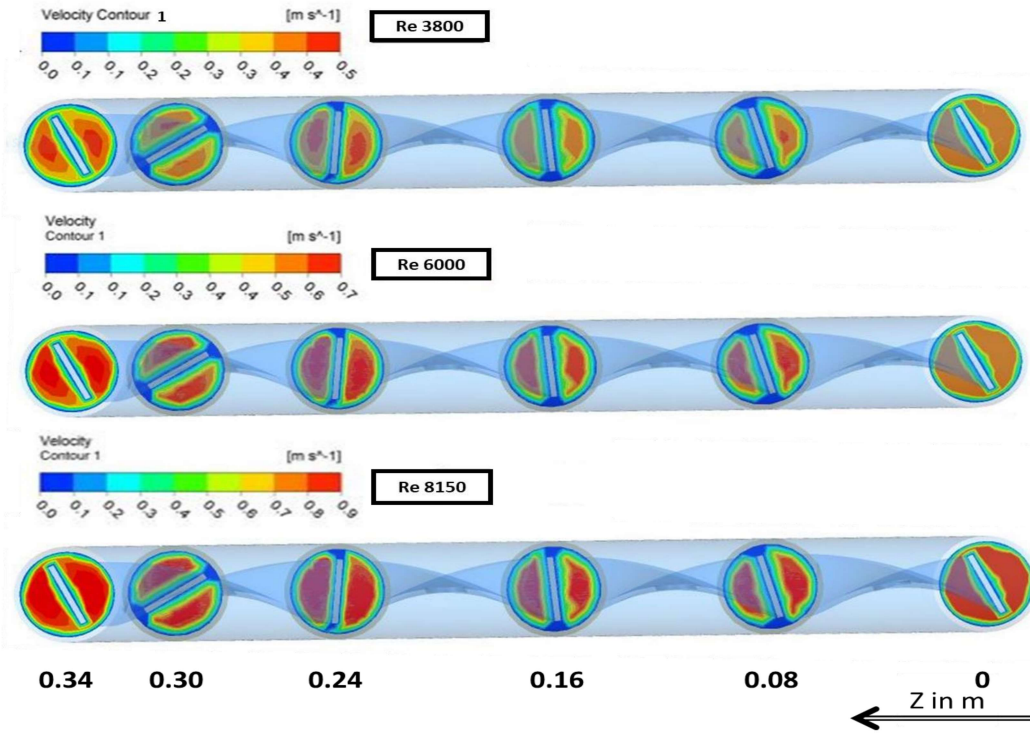

Fig. 6.8. Velocity contours with Reynolds number at different sections along the axial direction.

A lower perforated pitch allows the fluid to intermix frequently due to a larger number of perforations and thus results in a higher pressure drop. The pressure drop slope changes beyond Re of 6000 as the flow velocity is dominant at a higher Reynolds number. Lower perforated pitch, higher perforated diameter, and higher Reynolds number show larger pressure drop. PTTI in HX of different geometrical and fluid flow conditions augments the heat transfer but at the cost of pressure drop. Fig. 6.8 presents the axial velocity contour at six different positions in the longitudinal direction under three different fluid flow conditions. In each case, the twisted tape shows the swirl flow generation at the tube's inlet section (Z = 0m). Higher flow rate increases swirling and secondary flow to the fluid; see at location Z = 0.34m. Although the axial flow rates dominated the HX at a higher flow rate, reducing the time of contact of swirling near the tube wall and the twisted surface was a significant reason for the lesser temperature drop. The internal

surface of the tube wall and the twisted tape shows zero velocity due to the no-slip condition. The axial flow is due to mass flow rate while swirling occurs near the twisted surface curvature and the tube wall radially at each tube location (Fig. 6.8). However, the flow velocity variation with perforated diameter is shown in Fig. 6.9. Also, larger size perforation allows higher eddies and results in a better intermixing of fluid, and plays a crucial role insignificantly enhancing heat transfer and pressure drop.

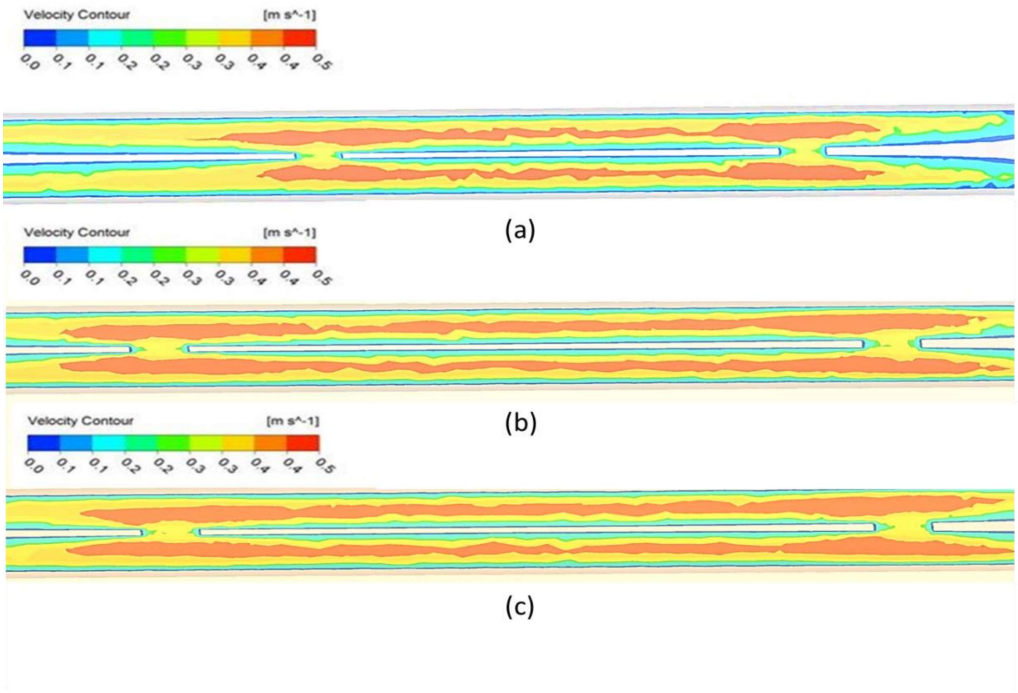

Fig. 6.9. Velocity contour at different perforated diameter, (a) 2mm; (b) 3mm; (c) 4mm.

To indicate the pumping cost requirement in the presence of PTTI in HX, friction ratio variation with PTTI geometry and fluid flow variation is presented in Fig. 6.10. The frictional reference factor is the outcome from the, and the frictional factor for PTTI in plain tube. From Eq. (6.18), the pressure drop in the numerator shows a direct growth in the frictional factor with the development of the numerator parameter. While in Eq. (6.18), a cubic velocity is at the denominator, and the impact of cubic velocity dominates pressure drop rise.

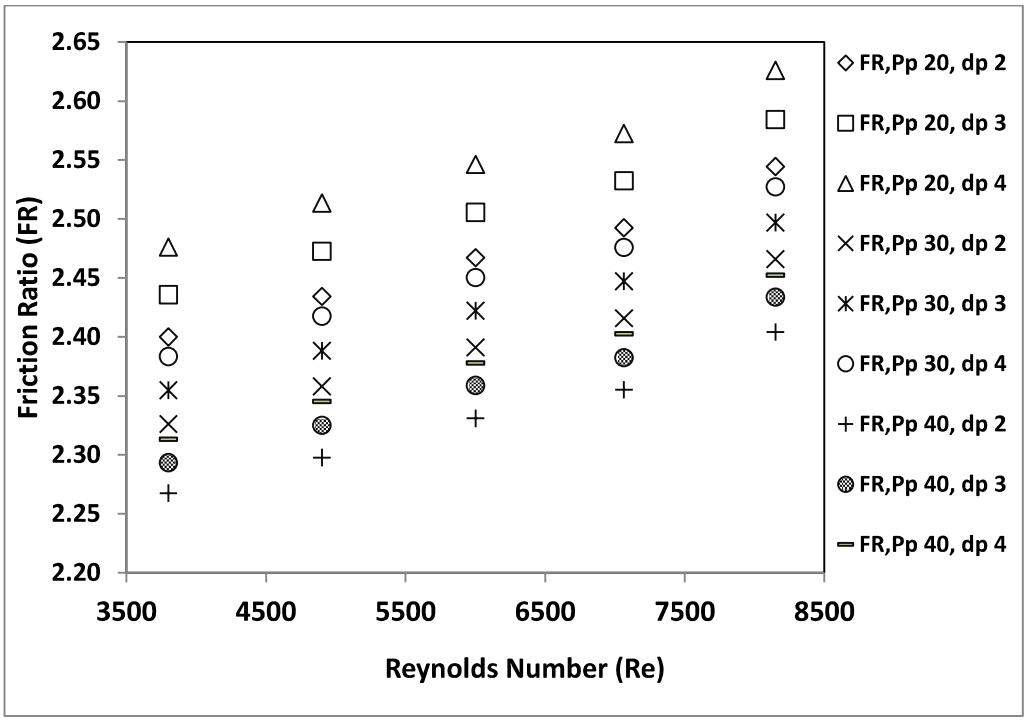

Fig. 6.10. Friction ratio with Reynolds number for different PTTI conditions.

However, when the Reynolds number increases, the friction ratio also increases and directly influences the perforated diameter and pitch of the PTTI. The smaller perforation size and higher perforated pitch have the lowest friction ratio, and the trend shows FR increases with perforation size enlargement and lowered perforated pitch. Geometrical and fluid flow variation shows remarkable FR for Re 3800 to 8150 friction ratio ranges from 2.26 to 2.63, respectively.

6.3.3 Effect of flow and geometrical parameters on OTP, DG CO_2, HXOC, and UA

The combined effect of heat transfer and pressure drop for a PTTI in HX is necessary, as twisted tape improves swirling and secondary flow, enabling heat transfer improvement and increasing pressure drop. A non-dimensional parameter, under constant pumping power, is defined as overall thermal performance (OTP) in Eq. (6.13). Lower pressure drop and higher heat transfer suggest a higher overall thermal performance or vice versa. Overall thermal performance with Reynolds number ranges from 3800 to 8150 under different perforated pitches, and size is presented in Fig. 6.11.

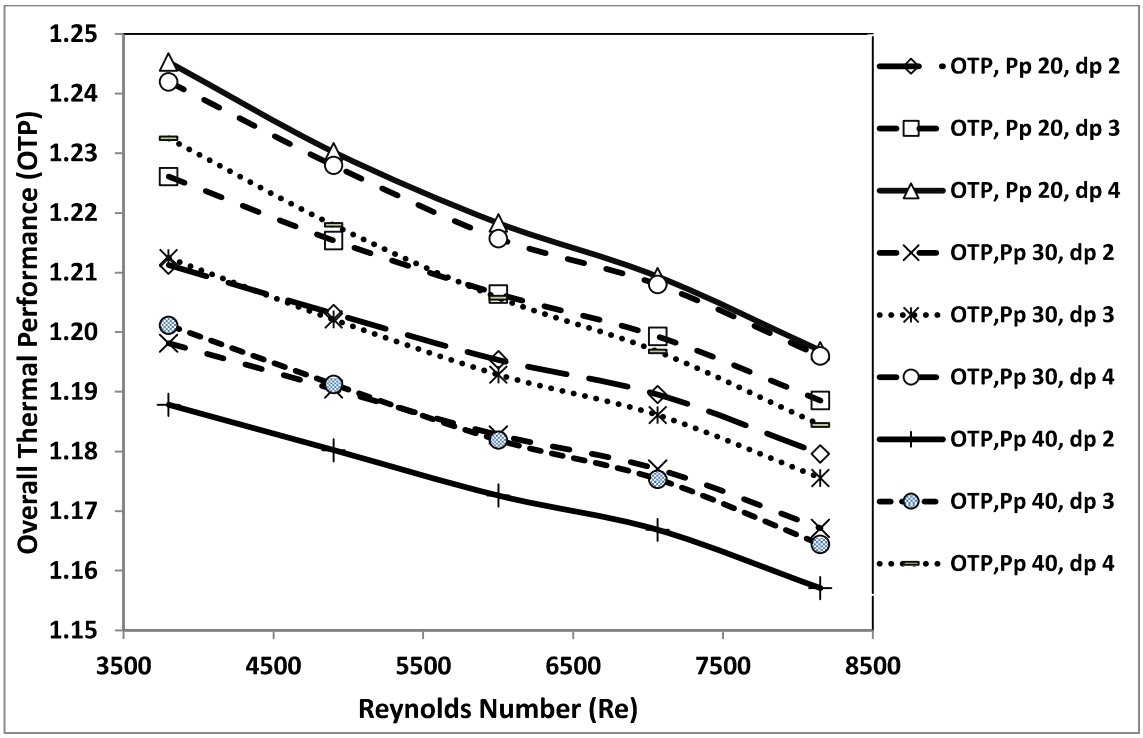

Fig. 6.11. OTP with Reynolds number for different PTTI conditions.

Considerable drop in OTP on Reynolds number increment, as higher flow rate shows the growth in pressure drop. The plot trend shows that at Reynolds number 6000, the curve changes are defined as critical Re. Beyond that, the OTP tends to drop rapidly due to the pressure drop dominating at a higher flow rate than the Nusselt number, and the critical point is observed in Fig. 6.11. This ensures the PTTI in HX should be a potential insert for heat transfer enhancement in lower Re, below 6000. Although, OTP is more significant than unity for all cases considered. Of the geometrical cases considered, the lower perforated pitch and higher perforation size combination show the highest.

In comparison, higher perforated pitch and smaller perforation size show the lowest OTP at all Reynolds numbers. With geometrical and fluid variation applied, OTP outcomes range from 1.16 to 1.25. OTP suggests PTTI in HX gives better thermal performance if it is operated below 6000 Re, and beyond that, the pressure drop is likely to be increased more for minor enhancement.

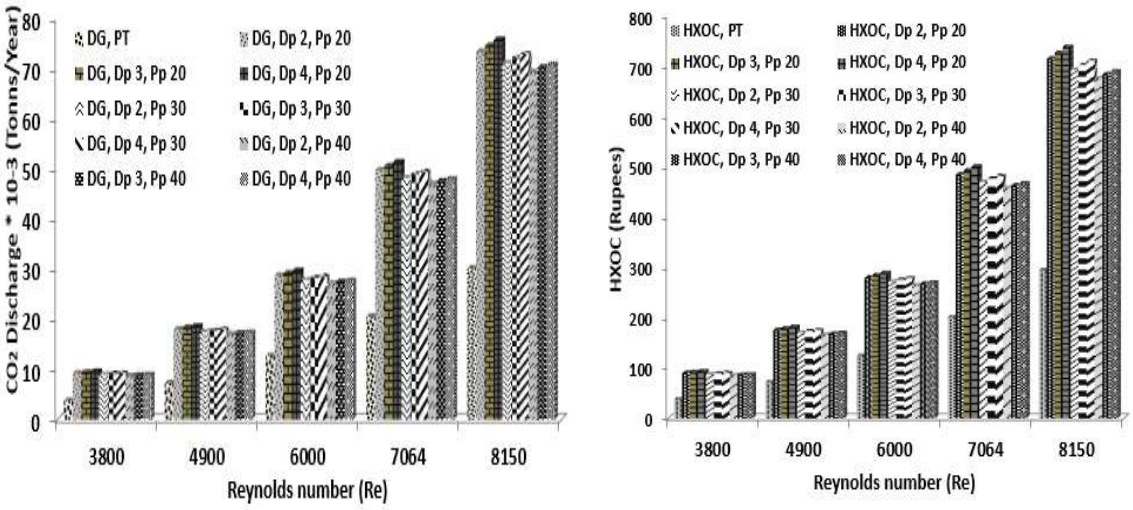

(a) **(b)**

Fig. 6.12. Heat exchanger of different PTTI, (a) CO_2 discharge with Reynolds number; (b) HX_{OC} with Reynolds number.

Furthermore, the PTTI in HX requires additional power consumption through coal combustion to run the HX efficiently. Discharge to the environment and HX operating cost for different PTTI geometry modifications with Reynolds number are shown in Fig. 6.12 (a) and Fig. 6.12 (b), respectively. The trend shows a similar pressure drop variation with flow rate. PTTI in HX operates for 365 days for 8 hours a day before maintenance and produces the lowest operating cost and carbon discharge to the environment at 3800 Re and increases with the flow increment. At critical Re 6000, a perforated diameter of 4mm and perforated pitch of 20mm produces 29.6kg of carbon discharge at 288 rupees to run HX for the entire year. Although the result shows higher thermal performance at higher flow rate costs additional CO_2 discharge to the environment and higher operating costs. Thus, using the PTTI in HX below the critical 6000 Reynolds number is advisable, with a suitable set of geometrical conditions.

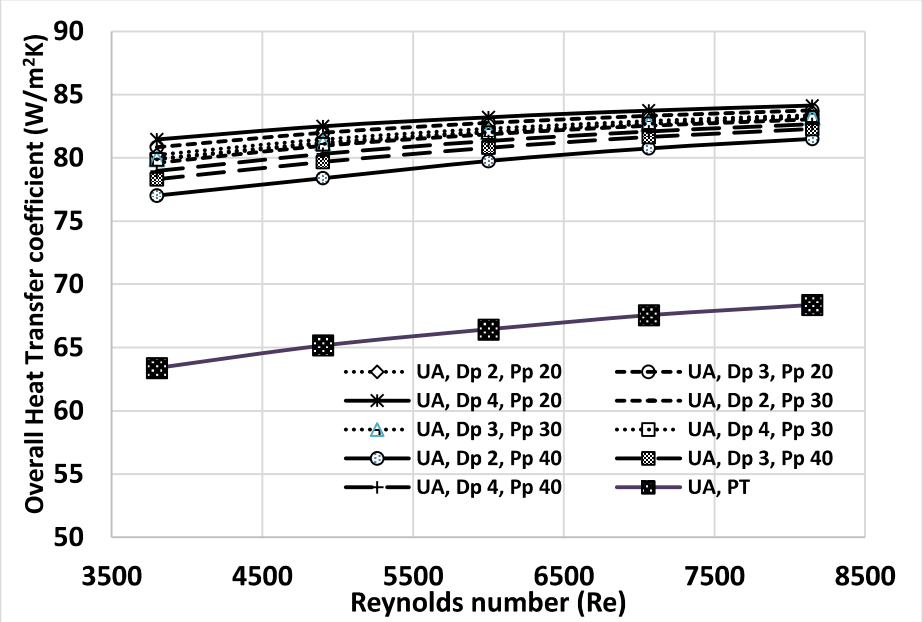

Fig. 6.13. Overall heat transfer coefficient with Reynolds number for different PTTI.

The utilization of tube inserts affects the heat transfer significantly. A parameter that considers both effects of internal (nanofluid) and external (air) fluid is the overall heat transfer coefficient (UA). However, air as an external fluid is kept constant, 5m/s [**Kumar et al. 2022**], and the UA variation with the internal nanofluid flow for different geometrical inserts is presented in Fig. 6.13. The UA is higher for the inserts. Due to the presence of inserts, the nanofluid heat transfer coefficient improved by providing secondary flows, increased fluid velocity, and better fluid mixing. For the set of geometry, D_p 4mm and P_p 20mm, at the lowest Reynolds number, 28.5% higher UA was obtained than without inserts. Lower inertia allows the fluid to have a higher resident time of fluid mixing near the wall and the twisted surface, thus ensuring more significant improvement. While for the case of D_p 2mm and P_p 40mm, 19.2% higher UA is obtained compared to without inserts. Therefore, the PTTI shows significant enhancement considering the external fluid as well.

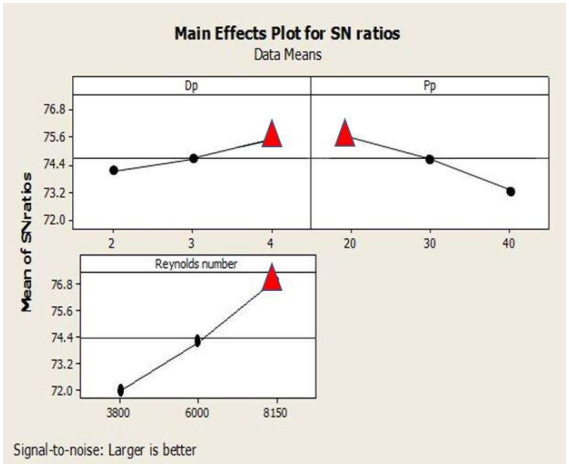

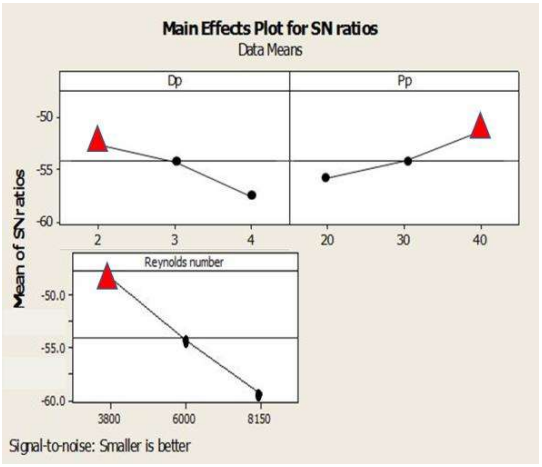

(a) **(b)**

Fig. 6.14. SN ratios, (a)Heat transfer coefficient (HTC), larger is better; (b) Pressure drop, smaller is better.

6.3.4 Effect of design parameters on heat transfer coefficient and pressure drop using Taguchi method

Response diagrams of the HTC and pressure drop concerning the factor and corresponding levels are shown in Fig. 6.14. The main objective is to be high heat transfer and low-pressure drop in HX; therefore, larger is better, and smaller is better considered for HTC and pressure drop, respectively. The higher slope in the SN ratio plot represents a significant and influential parameter for the objective. Therefore, D_p 4mm, P_p 20mm, and Reynolds number of 8150 influence HTC; for instance, see Fig 6.14 (a). Also, lower pressure drop can be achieved with D_p 2mm, P_p of 40mm, and at a lower Reynolds number 3800, as shown in the peak SN ratio plot; for instance, see Fig 6.14 (b). Although, the Reynolds number, fluid flow rate, is the most influential factor, followed by a perforated pitch and then perforated diameter.

Table. 6.6. SNR, normalized response, Grey relational coefficient, and grade with the preferred order of the HX.

Run	D_P	P_p	Re	SNR HTC	SNR (Δp)	Normalized Response		GRC		GRG	Order
						HTC	Δp	HTC	Δp		
1	2	20	3800	72.06	-48.29	0.037	0.982	0.342	0.966	0.654	3
2	2	30	6000	74.96	-54.75	0.482	0.598	0.491	0.554	0.523	8
3	2	40	8150	76.93	-59.16	0.880	0.112	0.807	0.360	0.584	6
4	3	20	6000	75.21	-55.12	0.527	0.566	0.514	0.535	0.525	7
5	3	30	8150	77.12	-59.46	0.926	0.070	0.871	0.350	0.610	5
6	3	40	3800	71.77	-47.84	0.000	1.000	0.232	1.000	0.616	4
7	4	20	3800	77.44	-59.93	1.000	0.000	1.000	0.333	0.667	1
8	4	30	6000	72.02	-48.21	0.031	0.986	0.340	0.972	0.656	2
9	4	40	8150	74.93	-54.70	0.476	0.602	0.488	0.557	0.522	9

6.3.5 Optimization of multiple responses using Grey analysis

In the Taguchi method, the SN ratio helps to determine each design parameter's influence on the individual target response. But when multiple responses mean combining all target responses for the optimization process, no single design satisfies all responses. Therefore, a systematic approach is needed, mainly Grey relational analysis, which will select the optimum design parameters to influence each target response.

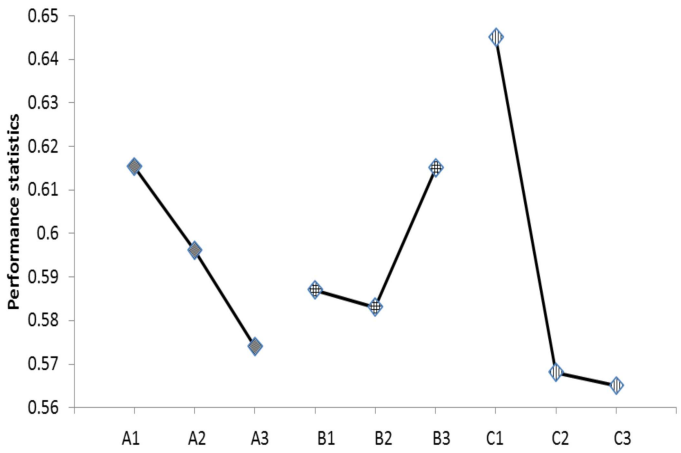

Fig. 6.15. Performance statistics with design parameters.

The target response is normalized using the theoretical value from 0 to 1. The Grey relational coefficient is analytically determined using Eq. (6.24), tabulated in Table 4.5. Grey relational grade (GRG) is determined using Eq. (6.25), assigned equal weightage to the target response for higher HTC and lower pressure drop. Rank is assigned, preferring the highest value of GRG as better for all the runs. However, performance statistics variations with the design parameters are illustrated in Fig. 6.15. Performance is highest on the Perforated pitch of low level (A1), the perforated diameter of high level (B3), and the mass flow rate of low level (C3). From GRG, the result reveals set of design parameters of the HX to operate under the assigned target response would be D_p 4mm, Pp 20mm, 3800 Reynolds number as most preferred ranked 1st and D_p 4mm, Pp 40mm, Reynolds number, 8150, as least preferred ranked 9th. Ranking allows users to choose a sagaciously different set of geometrical and fluid flow conditions to be prioritized to ease manufacturing and minimum operating cost with optimum working performance of the heat exchanger.

6.4 Highlights of the study

The present chapter focuses on numerical analysis of perforated twisted tape inserts in a tube heat exchanger with nanofluid as a working fluid in the turbulent regime with Reynolds number of 3800 - 8150. Effects of geometrical and fluid flow parameters are considered by utilizing nanofluid on the Nusselt ratio (NR), Friction ratio (FR), overall thermal performance (OTP), CO_2 discharge to the environment, and HXOC. Geometrical and fluid parameters influence heat transfer and pressure drop. Optimal process parameters for three different design factors (Reynolds number, perforated pitch, and perforated size) and their levels are analyzed using the Taguchi-Grey statistical tool for higher heat transfer and lower pressure drop. Necessary input requirements to carry out Taguchi-Grey investigations are carried out from CFD analysis. The following primary outcomes are:

- Low Reynolds number, below 6000, use of PTTI in HX is suitable for higher thermal enhancement, maximum 3.4% higher NR at Re 3800 compared to Re 8150.
- The fluid outlet temperature is obtained minimum at Re 3800 for all cases, and geometrical variation set P_p 40 mm, D_p 2mm and P_p 20mm, D_p 4mm of PTTI in HX achieved a maximum temperature difference of 3.12.
- PTTI in HX improvises overall heat transfer compared to plain tube, and the Overall heat transfer coefficient is 19.2 to 28.5% higher than plain tube due to PTTI in HX.
- The highest OTP of 1.25 is obtained for geometrical set P_p 20mm, D_p 4mm PTTI in HX at Re 3800, and decreases with the Reynolds number increment.
- The lowest FR of 2.26 is obtained for the geometrical set of P_p 40mm, D_p 2mm PTTI in HX at the lowest Re and increases with the flow increment.
- HXOC and CO_2 discharge requirements are 1.7 to 2.55 times more than the critical Reynolds number for optimal geometrical conditions.

- The most influential parameter for heat transfer and pressure drop is flow rate followed by a perforated pitch, and then the perforated diameter is obtained using Taguchi analysis.
- The geometric set of Pp 20mm, Dp 4mm, and Reynolds number 3800 fluid conditions is 1st priority obtained using Grey analysis and predicted the preference order for the set of geometrical and fluid conditions for higher heat transfer and lower pressure drop.
- P_p 40mm, D_p 2mm, and Reynolds number 8150 sets of geometrical and fluid conditions should be the least preferred predicted by Grey analysis.

This page is left intentionally blank